Correlated Electromagnetic Levitation Actuator: A Reaction Sphere-Based Attitude Control System

Sarah Triana[*] , Peter Weber[†] , Ryan Deters[‡]
NASA Marshall Space Flight Center, Huntsville, Alabama, 35808

Amy Huynh[§]
University of California, Irvine, Irvine, California, 92697

Kai Bailey[¶]
University of Washington, Seattle, WA 98195

To address problems experienced by current reaction wheels and control moment gyroscope-based attitude control systems (ACS), researchers at National Aeronautics and Space Administration's (NASA's) Marshall Space Flight Center (MSFC) have begun developing a reaction sphere actuator based on correlated electromagnetic levitation that will be immune to destructive bearing friction, momentum saturation, and gimbal lock. The Correlated Electromagnetic Levitation Actuator (CELA) advances the state of the art of reaction sphere ACSs by employing the concept of correlated magnetics. It is a frictionless, direct-drive reaction sphere that harnesses a unique technology with an array of applications across multiple disciplines. Correlated electromagnets function in a manner that is analogous to a matched filter; the convolution of two signals is peaked at the index representing the greatest match. For CELA, the signals are the patterns of magnetic flux density as a function of position. The magnitude of the convolution equates to an attractive or repulsive force, and these forces can be azimuthal or radial. The development of CELA is based in four distinct disciplines: Advanced Manufacturing, Prototype Development, Electromagnetic Modeling, and Controls. We are developing novel manufacturing techniques required to build arrays of permanent and electromagnet dipoles on curved surfaces. To print the permanent magnetic array, we have developed a probe with pyramidal magnets that will reside on a robotic arm to induce localized magnetic fields on a surface. We have also used high temperature ovens to erase dipole patterns from a permanent magnet by heating the surface to its Curie temperature. A number of test articles and prototypes have been developed using additive manufacturing methods. These prototypes have included hemispherical motors to test the drive algorithm, and a levitation test bed that demonstrates a magnetic bearing method based on attractive magnetic forces and ratiometric Hall effect sensors. We developed an array of electromagnetic dipoles on a printed circuit board (PCB) with individual H-bridges controlling each coil. This device created various flux density patterns and we measured their magnetic fields using a custom Hall effect 3-D probe and a LabVIEW virtual instrument. These data will serve as a benchmark for characterizing the accuracy of future models. Current work is focused on modeling the magnetic fields of our prototype arrays using COMSOL finite element analysis (FEA) and verifying the model against our test data. Accurate modeling will allow us to quickly test new patterns of electromagnets and their macro behavior. Eventually, the magnetic field models will be implemented in our controls simulations to facilitate precise control of the reaction sphere. Initial model results agree with field measurements to within 1 G ($\leq$5% of measured flux density). Currently, we are testing different material properties of the electromagnets and their magnetic fields and

[*]Principal Investigator and Project Manager, Advanced Concepts Office (ACO) at NASA Marshall Space Flight Center (MSFC).
[†]Power Electronics Design Engineer, Power and Electrical Integration Branch at NASA MSFC, and AIAA Senior Member.
[‡]Discipline Lead, Advanced Manufacturing at NASA MSFC, and AIAA Member.
[§]Undergraduate Student, Department of Mechanical and Aerospace Engineering, and AIAA Student Member.
[¶]Undergraduate Student, Department of Aeronautics and Astronautics.

thermal effects. These results will be used to refine the design of the electromagnetic dipoles. Our control efforts have centered on developing commutation, levitation, and field pattern shaping hardware in the form of breadboards and PCBs with software running on a local microcontroller. In addition, our partners developed MATLAB Simulink models to demonstrate a PID controller that mitigates disturbance forces resulting from the interaction of drive and levitation magnetics. Finally, we have designed a three-axis test stand that will be used in future work to demonstrate CELA's orientation control capability.

I. Introduction

CELA is a Correlated Electromagnetic Levitation Actuator, or a frictionless, direct-drive reaction wheel that harnesses a unique technology with an array of applications across multiple disciplines. CELA is intended to overcome current issues in attitude control systems (ACS): 1) it will remove the need for ball bearings that fail due to excessive friction, 2) it will circumvent momentum saturation, 3) it will not be limited by gimbal lock, and 4) it will eliminate the need for multiple devices to handle 3-axis attitude control. These issues will be discussed in detail in the following sections.

CELA replaces a mechanical bearing with electromagnetically coupled surfaces, using an array of miniature electromagnets that interacts with a patterned permanent correlated magnetic surface to create levitation and rotation. This technology can achieve many complex macro behaviors in addition to levitation: strong attach forces, rotational acceleration, braking, and more.

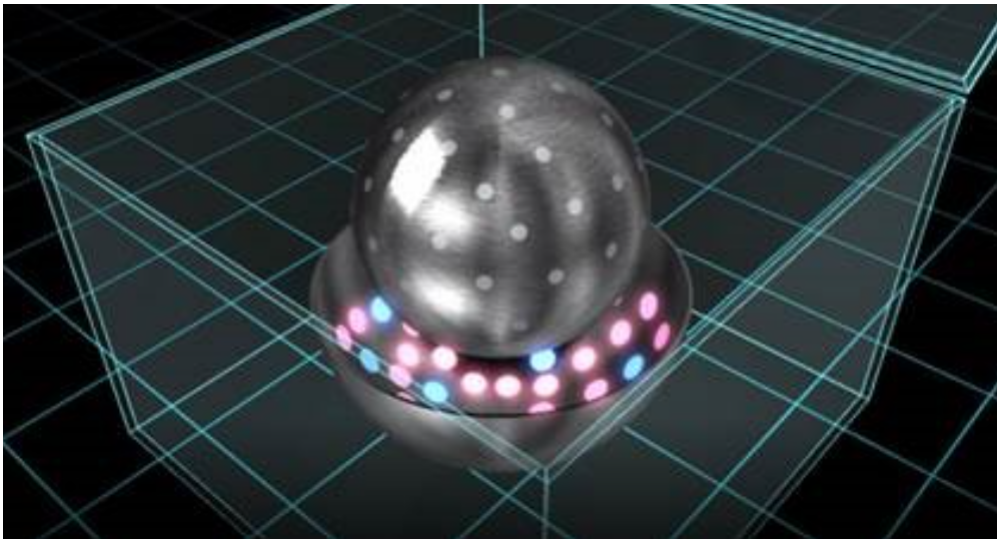

Fig. 1 CELA concept. Outer shell cutaway for illustrative purposes.

The final device will be a Reaction Sphere – a central spherical mass with magnetic dipoles printed on the surface that interacts with a surrounding hollow shell composed of electromagnetic dipoles. In addition to eliminating the need for ball bearings and mechanical systems, CELA removes the need for three reaction wheels to control the three spacecraft axes. Instead, the Reaction Sphere will be free to move in any direction, and hence control any axis needed to point the spacecraft. The use of advanced manufacturing to produce CELA will enable the next generation of high-performance, long-duration, reliable attitude control technology for future missions to the Moon, Mars, and beyond.

A. Electric Drive Trade Studies

In order to determine the appropriate drive mechanism for the Reaction Sphere, we considered the implications of a spherical magnetic bearing on the common types of motors. We analyzed two possibilities: coupled drive and bearing magnetics, and decoupled forces. In both cases, it was immediately clear that the design requires all active electronics to be on the exterior sphere, resulting in only permanent magnets or ferromagnetic materials on the interior rotating sphere. We also considered diamagnetic materials embedded in a paramagnetic structure, but this approach did not seem promising given the required magnitudes of forces. Presently we are pursuing drive and bearing mechanisms that are based on the interaction between permanent magnets and electromagnets. These can be attractive or repulsive, but repulsive forces require the use of electromagnets without ferromagnetic cores, otherwise the attractive magnetic reluctance minimization forces overwhelm the repulsive forces.

We considered induction drives, but were deterred by the complexity of the required spherical polyphase rotating flux. The inherent slip of an induction drive also would likely hinder efforts at singularity avoidance (discussed in section II). Switched or variable reluctance drives were rejected due to the saliencies on the rotor and stator, and the resulting harmonic content that would be induced in the vibrational spectrum. We rejected shunt & series wound brushed Direct Current (DC) motors because the brushes are not compatible with magnetic levitation and severely limit the motor lifetime. We settled on a method similar to a brushless DC motor with a permanent magnet rotor.

II. Limitations of the Current Technology

Spacecraft attitude control can be achieved by three-axis reaction or momentum wheels, control moment gyros (CMG), reaction control systems (RCS), differential photon pressure, magnetorquers, and other devices. The primary means of attitude control is often a set of reaction wheels for devices with low mass, and CMGs for high mass vehicles. Both of these techniques are generally favored over RCS for long duration missions because they do not require expulsion of propellant and are more fuel efficient. In addition, the reaction wheel or CMG provided torque allows more precise pointing control than thrusters, which can be important for scientific observation platforms such as telescopes and cameras. It is worth noting that reaction wheels are simpler to implement, while CMGs are more efficient, generating orders of magnitude more torque for a given input power.

An important limitation for reaction wheels and CMGs is that they are unable to provide attitude control indefinitely on their own. Reaction wheels are subject to a loss of attitude control due to momentum saturation, in which the wheel has reached its maximum speed and can store no additional angular momentum with which to steer the spacecraft. Control about that spin axis can only be regained by performing desaturation maneuvers using a secondary attitude control system such as magnetorquers or RCS. Control moment gyros suffer from gimbal lock, in which two axes of control have become aligned. The alignment of the two gimbals results in the loss of one degree of freedom, in which case the matrix defining the steering law becomes rank deficient, or singular. For this reason this failure mode is known as a singularity. Again, a secondary system must be brought to bear to restore full attitude control.

By combining reaction wheels and CMGs, it has been demonstrated that the two failure modes can be overcome. One means of achieving this result uses variable speed control moment gyros (VSCMG) to avoid saturation and singularities [1, 2]. The Reaction Sphere we propose is equivalent to the VSCMG solution, but with several additional advantages, which we outline in the following sections.

The current state-of-the-art for reaction wheels, CMGs, and VSCMGs require bearings and lubricants to reduce friction between the housing and a flywheel. A number of spacecraft have had missions cut short or altered due to reaction wheel failures. These include Fuse, Hayabusa, Dawn, Time, and Kepler, among others. The most plausible proximate cause for most of these issues was identified as a dry cage instability, in which degradation or loss of lubricant allows friction and heat to build, eventually leading to a catastrophic failure. It has been conjectured that the space plasma environment may have contributed to the increased friction by altering the lubricant properties and by surface roughening of the bearings due to electrical charging following coronal mass ejections and other space weather events [3]. These issues have largely been addressed in the newer generation of wheels, but the appeal of magnetic bearings continues to motivate their development and increased adoption [4].

A. Advantages of the Reaction Sphere

For clarity, we enumerate the advantages of the Reaction Sphere in this section.

1. Power & Mass Efficiency

As mentioned above, CMGs are more efficient when large torque outputs are needed. For this reason, they are generally used when spacecraft exceed a mass threshold. Reaction wheels have fewer components and are therefore lighter. For this reason, they are generally used on small spacecraft for which the additional mass is significant and the pointing torque requirements are lower. The reaction sphere is able to operate as a CMG or as a momentum wheel. It can perform high torque maneuvers by rotating its spin axis while maintaining a constant spin rate. It can perform low torque maneuvers by varying the rate of spin about an arbitrary axis. It can perform an angular momentum storage function for momentum-bias stabilization. It achieves these two capabilities while retaining the lower complexity and increased mass efficiencies of reaction wheels.

2. The Reaction Sphere is robust against saturation and gimbal lock.

Control algorithms can be devised that transition to reaction wheel type control when CMG singularities are approached and to CMG type control when desaturation is required. In essence, the extra degree of freedom imparted by varying the revolutions per minute (rpm) of the CMG flywheel permits singularity avoidance.

3. Simplified Control Laws

Reaction wheel control laws are simpler than CMG laws. The Reaction Sphere can perform CMG type torque generation with control laws that reduce to specification of a stepwise process of state transitions between spin axis orientation and rotation rates. The Reaction Sphere can improve pointing accuracy and algorithmic efficiency. Optimization of control creates an opportunity to develop new algorithms, including the use of unit quaternion-based control.

4. Maintenance

Conventional attitude control systems use contact bearings which sometimes fail before the mission is complete. Several spacecraft have had to modify or abort missions due to reaction wheel bearing failure. The Reaction Sphere uses frictionless magnetic bearings. The spherical symmetry potentially facilitates magnetic field modeling, design, and control. In other words, models can be developed for a single axis or magnetic circuit, and then extrapolated to a 3d device by repeated rotation about the polar and azimuthal angles θ and ϕ.

5. Manufacturability

Some elements of the Reaction Sphere can be 3D printed. For instance, permanent magnets can be printed in place on a spherical surface. Planar magnetics for drive and bearing coils can be printed using conductive inks.

III. Methods

Our development approach is broken into four disciplines: Advanced Manufacturing, Controls, Electromagnetic Field Modeling, and Prototyping. Each discipline was selected based on the key components of the overall design. Most importantly, we need to model the electromagnetic fields accurately to understand their interactions with each other

as the electromagnetic fields change their strength, polarity, and patterns. These models will feed into our controls simulation, another vital component of CELA's design.

We have followed a Test Driven Development and Agile Management approach consisting of 4-6 week test cycles, with a single objective per cycle, and weekly testing to ensure we achieve each objective before moving on to the next cycle (i.e. objective). This ensures we can pivot our direction as we learn from the testing. This approach is also well-suited for CELA because the research and development of each discipline can be studied in parallel to one another in small chunks. For a cycle, an objective is chosen, along with its key performance parameters (KPPs), a test plan is written, and finally hardware is built and tested. This order ensures we do not build excess hardware that does not accomplish our objective. Some of the objectives include characterizing the levitation and rotation, characterizing materials to produce more efficient electromagnets and miniaturize them, and base-lining the controls architecture. The majority of the work occurs in our onsite lab at Marshall Space Flight Center (MSFC), since CELA is a small technology development project.

Our current work focuses on modeling and simulating the electromagnetic fields of the Reaction Sphere using COMSOL. Accurate modeling is vital to informing the controls algorithm that needs to precisely control the spacecraft's attitude. In order to validate our models, we first modeled the original prototypes we had built and tested. These prototypes were 2-dimensional circuit boards, covered with an array of electromagnets (commercial off the shelf (COTS) inductors), each with a different pattern. We tested different dipole patterns in addition to the physical layout patterns, gathering information on magnetic field strength, current, temperature, and other factors. This is the data we used to match to our COMSOL model. After verifying our models, we modeled the levitation behavior from Correlated Magnetics Research, LLC's permanent magnets, looking at the field strength based on the plates' offset distance from each other. After verifying the electromagnetic and permanent magnetic data, we started to incorporate the dynamics of the plates interacting with each other. Finally, we started to build the model of the Reaction Sphere. No simulations have yet been completed on the Reaction Sphere COMSOL model.

Advanced Manufacturing studies so far have focused on developing the inner sphere, i.e. the rotor. The rotor will be constructed of magnetic material developed in-house, and will include printing dipoles on the entire surface of the sphere. The dipole pattern on the rotor will interact with, be controlled by, the array of correlated electromagnets on the outer sphere, i.e. the stator. To rapidly test different dipole patterns from our electromagnetic field models, we need to be able to quickly print rotor prototypes with those patterns. To do this, we can either build a new magnetic spherical rotor without polarities and then print the dipoles on the surface, or we can reuse the previous rotor, wipe the current polarities, and reprint a new polarity pattern on the surface. Currently, we have focused on the latter. We have used various methods to wipe the magnetic surface of a 2D correlated magnetic array. We have also started some research on manufacturing the outer sphere, the stator, focusing on printing tiny electromagnets using liquid silver and filling spiral traces.

Prototyping involved various test set ups throughout many sprints and cycles. Initially, tests were created to stably levitate a flat plate of correlated magnetic dipoles, using 3D printing and tiny magnets embedded in the surface. Then, we built a 3D printed hemisphere with permanent magnets attached to its rim and used a Hall Effect sensor to track the rotation as the hemisphere spun, as well as the balance of the hemisphere. Then, we moved on to a full sphere prototype, focusing on single axis levitation first. To stably levitate the axle in one dimension, a test set-up was conducted to use an electromagnet that attached to the prototype in the zenith position, and an axle with a single magnet attached to its end. Next steps include adding magnets to the bottom of the prototype and axle, adding a second electromagnetic coil in the Nadir position, and re-tuning the proportional–integral–derivative (PID) values to accommodate all of the changes. We will continue to modify and add electromagnets and modify the axle to add complexity and test 3D rotational control of the axle.

Our controls simulations focus on separating the levitation magnetics from the rotational magnetics. Once we can effectively model each behavior independently, we will combine the two models into one final simulation to control the Reaction Sphere. Currently, our development has focused on the levitation of an iron inner sphere (rotor), by an external sphere (stator). The stator is made up of electromagnets that levitate the iron rotor. The inner sphere contains dipoles printed on the surface of the iron, which acts as disturbance forces to the stator. The dipoles represent the correlated magnet pattern that will be acted upon by the stator's correlated electromagnets for rotational control. Modeling the dipoles as disturbances allows us to separate the levitation from the rotational control. We will continue to increase the

number of dipoles on the surface until the entire surface of the rotor is covered in a pattern of dipoles, which will match the final prototype. The number of electromagnetic dipoles on the stator will also be increased. After a full model of the levitation has been completed, our focus will shift to the rotational control of the rotor of correlated magnets by the stator of correlated electromagnets, focusing on the patterns necessary to effectively and precisely point the rotor.

IV. Prototypes

A. 2D Electromagnet Array

The initial project phase involved the development of 2-dimensional prototypes. The purpose of this phase was to extend the concept of correlated magnets to electromagnets. This required the ability to turn them on and off, change their polarity, vary their strengths, and generate patterns. The electromagnets were through-hole mounted inductors of ~1300 turns of 38 AWG wire wound on a ferrite core. Prior to this point, the usefulness of correlated magnetics had been demonstrated with permanent magnets. A prototype of a Correlated Electromagnetic Levitation Actuator (CELA) printed circuit board (PCB) was fabricated to demonstrate the value of replacing fixed patterns with programmable ones. Several different array geometries were developed, see Figure 3.

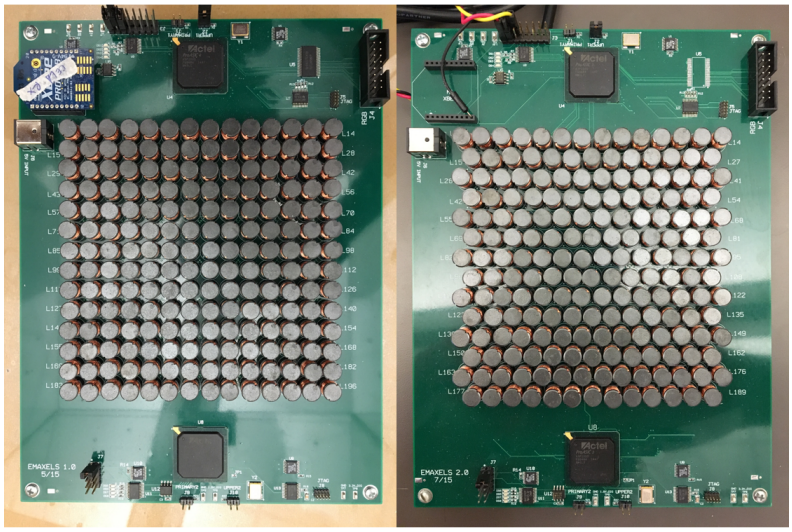

Fig. 2 Square and Staggered Inductor Arrays

The prototype PCBs accept power through a DC barrel jack, and communicate with the host computer through serial communication via a universal serial bus (USB) connection. The prototype was designed using programs within the Mentor Graphics electronic design suite. The prototypes were fabricated by a commercial PCB manufacturer and populated in-house. Several tests were performed with varying magnetic field patterns. A 3D printer was leveraged as a mount for a scanning gaussmeter probe used to measure the magnetic field at discrete points above the electromagnet array.

The printer, gaussmeter, and CELA prototype were connected to the computer via USB and controlled using a LabVIEW virtual instrument (VI) and a Python script. The temperature was measured by establishing a live video link with a thermal camera and recording the maximum temperature throughout the test, and an Arduino microcontroller and current sensor were used to measure the power consumption during the test; the temperature and power measurements were recorded with the same script used to control the printer. The results, test parameters (measured area, distance from array, etc.), and array configuration were recorded, and the magnetic field strength distribution, temperature, and power consumption were plotted as functions of time and position using MATLAB.

B. Spherical Motor

The spherical motor prototype concept is shown in Figure 3, and one early physical realization is shown in Figure 4. The device is designed to allow it to be expanded in subsequent iterations to allow finer resolution of the rotational axis. Each of the circular holes on the outer rings is threaded to accomodate a custom 3-d printed electromagnet wound on a polylactic acid (PLA) core.

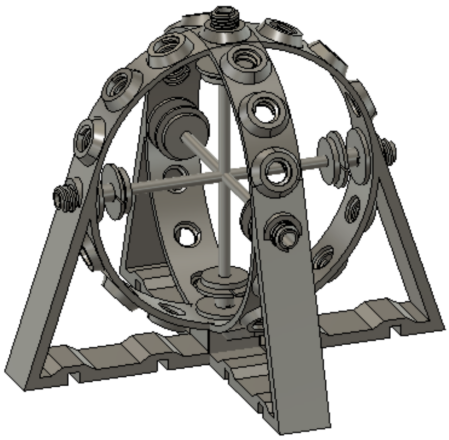

Fig. 3 Spherical Motor 3-d Model (inner sphere not shown)

The device shown in Figure 3 was 3-d printed and used to develop the circuitry for the magnetic levitation. The physics controlling the bearing forces are discussed in Section V.B. The software controlling the coil current runs on an Arduino microcontroller, which performs pulse-width modulation (PWM) control of the metal–oxide–semiconductor field-effect transistor (MOSFET) gates in series with the levitation coil.

Fig. 4 Early Reaction Sphere Levitation Test Rig

V. Analysis

A. 2D Electromagnetic Array

Following the magnetic flux density measurement by the custom scanning gaussmeter, a finite element analysis (FEA) model was generated and analyzed while performing parametric sweeps of the coil current and inductor bobbin core permeability. The results from the FEA were compared with the experimental data and the root mean squared (RMS) error (RMSE) minimized as a function of the swept parameters. The agreement between measurement and

analysis serves as a benchmark for future project phases, when time-varying flux density patterns with finer resolution will be required.

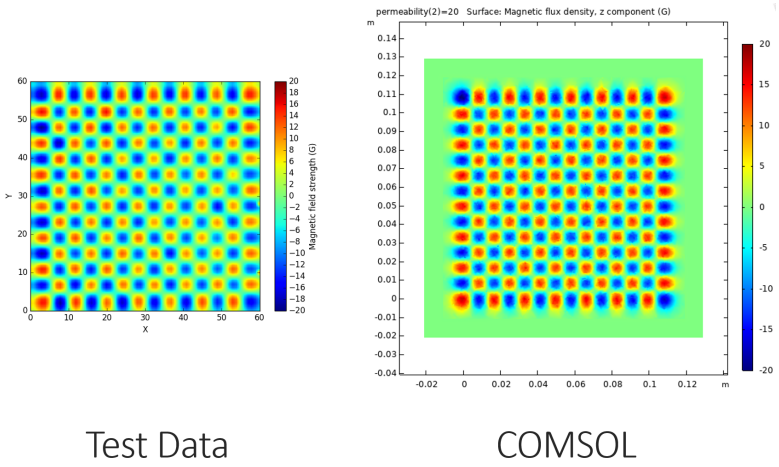

Fig. 5 Experimental magnetic field measurements vs FEA results

The FEA model began with a coil geometry imported from a CREO .prt file supplied by the vendor of the inductors used on these PCBs. This part was then arrayed as a 14 x 14 grid with the same dimensions as the PCB. We then added "Coil" physics to each of the 196 coils, alternating the setup so that half of them were negative and half were positive. The "Conductor model" was set to "Homogenized multiturn", and "Coil current" and "Number of turns" were specified as variables. We set the "Coil type" to "Circular". Following the completion of the study, we created a number of "Cut Planes" under the "Datasets" tab at 4, 5, 6, 7, and 8 mm above the electromagnets for comparison with the measured data. The results of the FEA study are shown alongside the measurements in Figure 5.

B. Magnetic Levitation Development

The spherical prototype consists of a disk with azimuthal magnets representing a 'latitude' line on the sphere. These are the rotor drive magnets. There are also magnets located at the top and bottom of a shaft fixed to the disk; these are the rotor bearing magnets. Both the rotor drive and bearing magnets are permanent NdFeB cylindrical type with axial fields. These magnets interact with stator solenoids. This section addresses the specifics of the bearing solenoids.

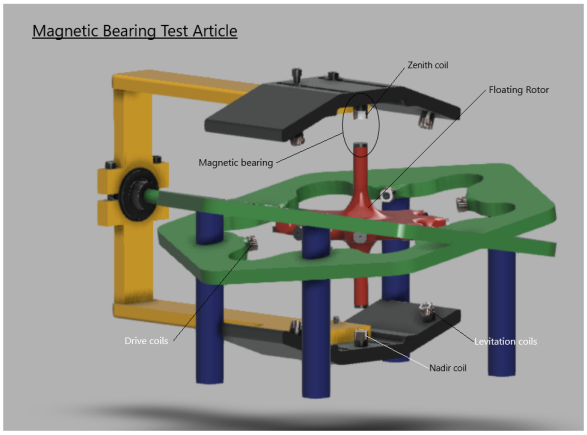

Fig. 6 Gimbaled Levitation Test Article Concept

The top bearing solenoid is hereafter referred to as the "Zenith Coil", and the bottom solenoid is the "Nadir Coil".

See Figure 6. In order to suspend the rotor, an attractive force between the bearing coils and the rotor magnets is produced by applying current to the two coils. The currents are balanced using a proportional-integral-derivative (PID) controller applying the gate voltages to field-effect transistors (FETs) in series with the coils and a current supply. The feedback signal used by the PID controller is produced by a ratiometric Hall effect sensor mounted in the center of the coil. The attractive force must be greater than any forces due to acceleration in order to maintain the rotor's position. In a static terrestrial test scenario, the rotor can be oriented such that the acceleration due to gravity pulls the rotor down, and the Zenith coil pulls it up, in which case the Nadir coil can be left de-energized. We begin with this scenario.

The rotor has a mass m_r kilograms, and permanent magnets located at the top and bottom have a diameter d_m meters, height h_m meters, and surface magnetic flux density B_m Tesla. The Zenith coil consists of an air core* solenoid, with diameter d_c meters, height h_c meters, and N turns. The supply can source up to I ampere of current through the coil windings. The Lorentz force on a charged particle due to a magnetic field is $\overrightarrow{F} = q\overrightarrow{v} \times \overrightarrow{B}$ Newtons, where $\overrightarrow{v}$ is the velocity of the charge carriers q. In the coil, current is confined by the coil windings to circulate such that the force produced is directed axially. The coil is held stationary, and the rotor is free to move, therefore the force will result in movement of the rotor, and the total force on the rotor $|F_r|$ can be expressed as:

$$|F_r| = |B_m(z)|I \cdot l \tag{1}$$

where $|B_m(z)|$ is the magnetic field due to the permanent magnet at the axial distance z meters between the coil and the rotor, and the total length of the coil is $l = \pi d_c N$ meters. Note: the following calculation neglects the effect on the magnetic field due to the height of the coil†.

To determine the field at the coil location, we use the following formula for the scalar potential [5]:

$$B_m(z) = \frac{\mu_0 M}{2}\left(\frac{z}{\sqrt{z^2 + \frac{d_m^2}{4}}} - \frac{z - h_m}{\sqrt{(z - h_m)^2 + \frac{d_m^2}{4}}}\right) \tag{2}$$

where μ_0 is the permeability of free space and M is the volume magnetization of the Neodymium magnet, assumed uniform and axial such that $\overrightarrow{M} = M\hat{k}$. We assume a rotor bearing comprising 8 stacked magnets [6] with parameters shown in Figure 7. We further assume a desired bearing clearance of 1 cm, and a maximum coil power dissipation of 1 Watt. The coil will heat up due to resistive dissipation, generating "copper losses" of $I^2 R_c$ Watts, where R_c is the coil resistance due to the wire gauge and length. This heat will require a means of removal for continuing coil operation.

Dimensions: 1/4" dia. x 1/32" thick
Tolerances: ±0.004" x ±0.004"
Material: NdFeB, Grade N52
Plating/Coating: Ni-Cu-Ni (Nickel)
Magnetization Direction: Axial (Poles on Flat Ends)
Weight: 0.00665 oz. (0.189 g)
Pull Force, Case 1: 0.66 lbs
Pull Force, Case 2: 4.33 lbs
Surface Field: 1795 Gauss
Max Operating Temp: 176ºF (80ºC)
Brmax: 14,800 Gauss
BHmax: 52 MGOe

Fig. 7 Nd52 Magnets used for levitation test article

The levitation coil inductance will determine the appropriate switching frequency, and in turn constrain the control loop frequency response. This inductance is given by:

$$\mu_0 N^2 \pi \frac{d_c^2}{4h_c} \tag{3}$$

*Air core solenoids are used to avoid reluctance-minimization forces

†The field experienced by circulating charge carriers at the windings closest to the magnets is greater than at those that are farthest. We assume this difference is not significant, but it lowers the total force for a given current, and we operate with margin to account for this error.

And the resulting maximum switching frequency f_{max} will be given by:

$$f_{max} = \frac{V_{exc}}{L\Delta I} Hz \tag{4}$$

where V_{exc} is the coil excitation voltage, L is the inductance, H is Henry, and ΔI is the range over which the coil current will be permitted to vary.

description	label	value	units	
magnetization	M	1177746.58	A/m	
axial distance*	z	1.64E-02	m	*from magnet bottom
magnet height	h_m	6.35E-03	m	
magnet radius	R	3.18E-03	m	
vacuum permeability	uo	1.2566E-06	H/m	
volume magnetization	uoM	1.48	T	
number of magnets	number	8		
surface field		0.66187612	T	
Bearing clearance	d	1.00E-02	m	
Axial field	B(z)	2.11E-02	T	
coil current	i	1.3	A	
coil height	h_c	8.00E-03	m	
coil diameter	d	8.00E-03	m	
number of turns	N	100	turns	
length	l total	2.51E+00	m	
coil resistance	R_c	0.4	ohms	
coil power	P_c	0.676	Watts	
coil inductance	L_c	7.8957E-05	H	
max PWM frequency	f_max	25330.2959	Hz	
operating voltage	V_op	1	V	
Delta current	delta_I	0.5	A	
force	Bil	6.90E-02	Newtons	
max weight	m	7.04E-03	kg	
		7.04E+00	g	
		2.48E-01	oz	

Fig. 8 Spreadsheet for calculating maximum levitated weight

The spreadsheet in Figure 8 shows the maximum weight that could be supported at a specified distance and current. In this case, an operating point of 1.3 ampere with $\delta I = 0.5$ ampere results in a max PWM operating frequency of $f_{max} \approx 25$ kHz, due to the chosen operating voltage and the coil inductance. The purpose of these calculations is to assist with determining the appropriate operating parameters for the magnetic bearing.

VI. Advanced Manufacturing

We have also developed several techniques under the rubric of Advanced Manufacturing. One of these methods involved attempts to erase dipoles from a magnetized neodymium plate. In order to achieve this, a Curie temperature of 320 degrees Celsius needs to be reached. First, we used a cartridge heater focused on the center of a single dipole. This proved ineffective due to conduction of the heat across the surface of the plate. An inductive heating source may prove more effective in concentrating the heat-affected zone and thereby reducing the effects of thermal conduction. The thickness of the plate also plays a factor in preventing heat transfer through the axis of the dipole.

Using a belt furnace, several neodymium plates were heated to 250, 400, and 850 degrees Celcius. All plates were placed in the furnace for 1.5 hours at each temperature. At the conclusion of the 250 degree test there was no change in magnetic pattern or in the appearance of the plates. At the conclusion of the 400 degree test, the magnetic pattern was completely erased and there was a change of appearance, but no physical damage was observed. At the conclusion of the 850 degree test there was a drastic change in magnetic pattern, plate appearance and structure. The 850 degree test

resulted in visible damage to the plate coating with the coating flaking off as well as powder indicating damage to both the coating and the underlying magnetic material.

Our next step will be to subject the neodymium plates to a concentrated magnet such as a pyramid magnet. With this approach, we will attempt to selectively magnetize the neodymium plate. The device will consist of a UR3 robot with an end of arm tool (EOAT) equipped with a motor, ethernet communication, and a pyramidal magnet. For context, we expect the EOAT to weigh less than 6.6 pounds. It should move to the proper location, and extend the pyramid magnet close to the surface of the plate to selectively magnetize the neodymium plate. The stepper motor would then retract the magnet before moving to the next location so as to not overdrive the robotic arm motors. The pull force of the magnet is estimated to be 287 N, if the magnet is allowed to make physical contact with the plate. A thin protective layer surrounding the pyramid magnet will prevent this from occurring. Our additive manufacturing lab also has the ability to print a variety of semiconductive inks on a surface including copper and silver. The printhead unit can be attached to a robotic arm to allow for movement in all five axes.

VII. Controls

We use the plant model shown in Figure 9 to develop the control algorithms. The goal is to monitor and control the spherical actuator's orientation angles $\theta\ \phi\ \psi$, rotational velocities $\dot{\theta}\ \dot{\phi}\ \dot{\psi}$, and absolute position $x\ y\ z$ to achieve the desired spacecraft Euler angles $\alpha\ \beta\ \gamma$. The sphere's absolute position is used as feedback for the magnetic levitation coils.

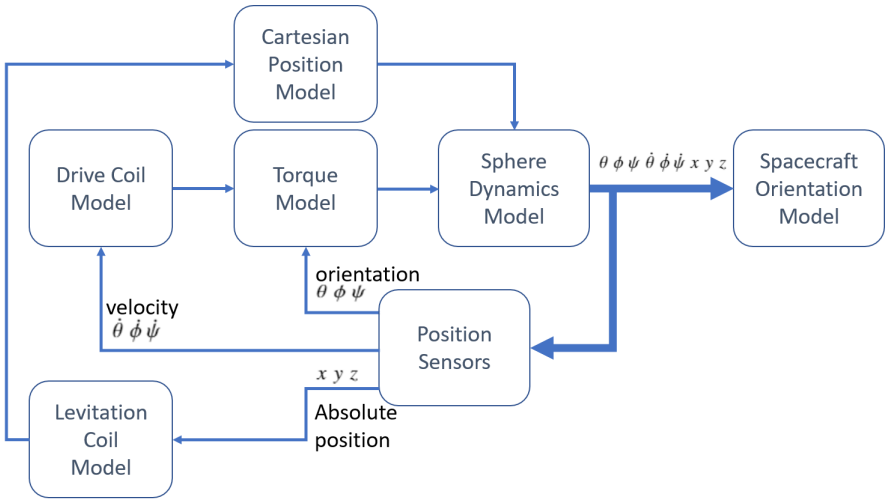

Fig. 9 Plant Model of Reaction Sphere with Decoupled Bearing Magnetics

We are given an initial orientation $\mathbf{E_i}$ and a desired final orientation $\mathbf{E_f}$, and we assume that the time to achieve the orientation adjustment is Δt:

$$\mathbf{E_i} = \begin{bmatrix} \alpha_i \\ \beta_i \\ \gamma_i \end{bmatrix} \qquad \text{and} \qquad \mathbf{E_f} = \begin{bmatrix} \alpha_f \\ \beta_f \\ \gamma_f \end{bmatrix} \tag{5}$$

The angular velocity vector $\boldsymbol{\omega}$ is then:

$$\boldsymbol{\omega} = \frac{d\mathbf{E}}{dt} = \frac{\mathbf{E_i} - \mathbf{E_f}}{\Delta t} \tag{6}$$

From this we obtain the necessary torque $\boldsymbol{\tau}$ as:

$$\boldsymbol{\tau} = \frac{d\mathbf{L}}{dt} \tag{7}$$

where $\mathbf{L} = \mathbf{I}\boldsymbol{\omega}$ is the angular momentum, and $\mathbf{I}$ is the moment of inertia tensor, expressed in terms of the Euler angles such that the tensor is a diagonal matrix with the principle moments of inertia appearing on the diagonals:

$$\mathbf{I} = \begin{bmatrix} I_x & 0 & 0 \\ 0 & I_y & 0 \\ 0 & 0 & I_z \end{bmatrix} \tag{8}$$

With appropriate transformations of coordinate frames, we obtain a rotational velocity vector ω:

$$\boldsymbol{\omega} = \begin{bmatrix} \omega_x \\ \omega_y \\ \omega_z \end{bmatrix} \tag{9}$$

Euler's rotation equations are then stated as:

$$\mathbf{I}\dot{\boldsymbol{\omega}} + \boldsymbol{\omega} \times \mathbf{I}\boldsymbol{\omega} = \boldsymbol{\tau} \tag{10}$$

where

$$\boldsymbol{\tau} = \begin{bmatrix} \tau_x \\ \tau_y \\ \tau_z \end{bmatrix} \tag{11}$$

is the torque vector required to achieve the desired spacecraft orientation. One advantage to the reaction wheel approach to this orientation change is the inherent simplicity of a linear combination of applied torques for achieving the result. For initial test purposes, the CELA reaction sphere will take this simple approach, while being held in a custom three-axis test fixture shown in Figure 10.

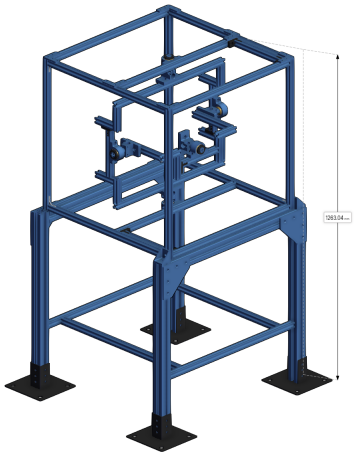

Fig. 10 Proposed test fixture for early Reaction Sphere iterations.

As mentioned in the Methods section, the initial Controls simulations focused on the levitation of the iron rotor by the electromagnetic stator. This was accomplished by first looking at a single electromagnet interacting with an iron sphere as shown in Figure 11a and Figure 11b. This configuration was modeled in COMSOL, see Figure 11c. COMSOL was used to calculate the magnetic force based on the current input and gap between the sphere and the electromagnet.

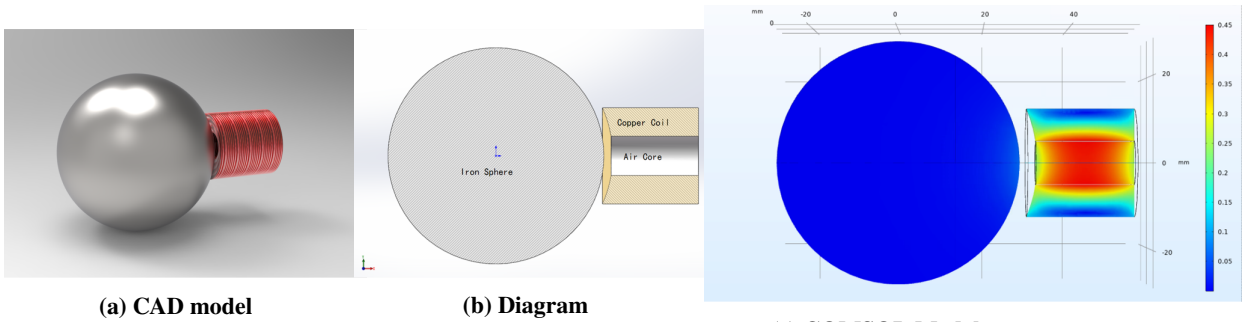

(a) CAD model **(b) Diagram** **(c) COMSOL Model**

Fig. 11 Iron Sphere and Air Core Electromagnet

From this, we were able to create a lookup data table that can be used in the control model to determine the position of the Reaction Sphere, Figure 12. What we can see in Figure 13 is that as the distance decreases, the magnetic force increases as we expect. As the magnitude of the current increases, so does the force, again as expected; when you have more current flowing through the coils, you have a stronger electromagnet, and hence a stronger magnetic attraction or repulsion force, depending on the direction of the current. For this data, a 4th degree polynomial fit works nicely, and was used to interpolate the data. This relationship was used to inform the position of the rotor with respect to the stator.

Gap Size	0	0.5	1	1.5	1.91	2	2.5	3	3.5	3.81	mm
Coil Current											
-10.000	11.2590000	9.3521000	7.8420000	6.5592000	5.7023000	5.5023000	4.6896000	4.0132000	3.4611000	3.1722000	
-5.000	2.8147000	2.3380000	1.9605000	1.6395000	1.4256000	1.3756000	1.1724000	1.0033000	0.8652800	0.7930600	
-2.000	0.4503400	0.3740800	0.3136800	0.2623700	0.2280900	0.2200900	0.1875800	0.1605300	0.1384400	0.1268900	
-1.000	0.1125900	0.0935210	0.0784200	0.0655920	0.0570230	0.0550230	0.0468960	0.0401320	0.0346110	0.0317220	
0.000	0.0000000	0.0000000	0.0000000	0.0000000	0.0000000	0.0000000	0.0000000	0.0000000	0.0000000	0.0000000	
1.000	0.1125900	0.0935210	0.0784200	0.0655920	0.0570230	0.0550230	0.0468960	0.0401320	0.0346110	0.0317220	
2.000	0.4503400	0.3740800	0.3136800	0.2623700	0.2280900	0.2200900	0.1875800	0.1605300	0.1384400	0.1268900	
5.000	2.8147000	2.3380000	1.9605000	1.6395000	1.4256000	1.3756000	1.1724000	1.0033000	0.8652800	0.7930600	
10.000	11.2590000	9.3521000	7.8420000	6.5592000	5.7023000	5.5023000	4.6896000	4.0132000	3.4611000	3.1722000	

Fig. 12 EM Force, Current, Distance Data Table

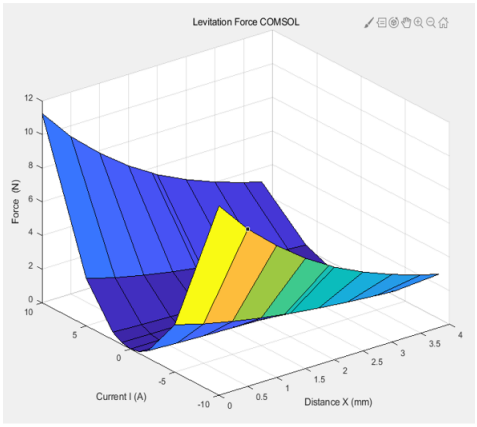

Fig. 13 Force, Current, Distance Relationship

Now that we understand the relationship between the rotor and the stator, we can use that data for our levitation controls simulation, Figure 14. The stator here is simplified as 6 electromagnets. The red dots are dipole disturbances that represent the array of correlated magnetic dipoles that would be used for rotational control, allowing us to decouple the levitation magnetics from the rotational magnetics.

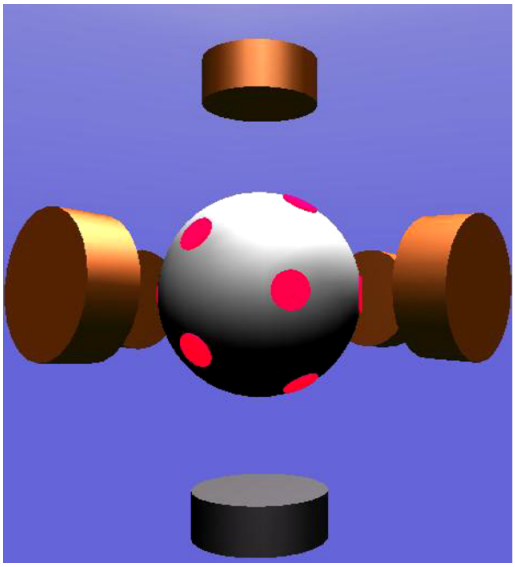

Fig. 14 Levitation Simulation

In the end, both the levitation and rotation would be controlled by the same magnetic dipoles, and these dipoles would eventually completely cover the surface of the rotor and stator, creating a higher density of dipoles over the surface, giving us better resolution, precision, and control.

VIII. Future Work

At present, a number of prototypes have been developed to advance the techniques used in the CELA concept. These prototypes remain useful for continued conceptual development. For instance, the programmable inductor arrays shown in Figure 2 can be mounted in a fixture with a fixed axial distance to a patterned permanent magnet plate, and the array coils can be energized through their dedicated H-bridges in a time-varying fashion. Leaving the permanent magnet plate free to rotate by attaching it to the axial locator shaft by means of a bearing, the plate can be induced to rotate. With this fixture, the rotational control circuitry and algorithms can be refined.

Another prototype that will continue to be used in the future is the spherical levitation actuator. This device was developed with a single zenith coil, while the action of the nadir coil was replaced with the force due to gravity. This device was used to achieve successful magnetic levitation with PWM coil control and ratiometric Hall effect sensing. However, the levitation coil was not given adequate thermal relief, and this will be addressed in a future upgrade. In addition, the nadir coil will be added to the setup, followed by a more advanced levitation test article consisting of six levitation coils representing three orthogonal axes.

The long term goal will be to develop a device that does not make a physical distinction between the levitation and drive magnetics. In other words, the two functions will be interchangeable. With this future device, we will explore the implications of hybrid control algorithms that blend the three axis flywheel concept with the gimbal-induced precession torque of a CMG. Finally, we will work to translate control algorithms from the Euler angle paradigm to one based on unit quaternions [7].

IX. Partnerships

We would like to acknowledge our invaluable collaboration with Professor Hector Gutierrez of the Florida Institute of Technology (FIT) for his work on the controls system and reaction sphere simulations.

Hector Gutierrez is our controls subject matter expert. He received his Ph.D. degree in Electrical Engineering in 1997 and M.Eng. Degree in Manufacturing Systems Engineering in 1993, from North Carolina State University, Raleigh. Gutierrez also received the B.Sc. Degree in Applied Mathematics from Universidad Cayetano Heredia, Lima, in 1989, and B.Sc. Degree in Mechanical Engineering from the Pontificia Universidad Catolica del Peru in 1991. He has been with the Department of Mechanical and Aerospace Engineering, Florida Institute of Technology since 1999, where he is currently a Professor. Gutiérrez received the National Science Foundation CAREER Award in 2001 and the Office of Naval Research Young Investigator Award in 2003 for his work in magnetic suspension systems, in motion control of multi-DOF servo levitation and stabilization of EDS electromagnetic launch, respectively.

X. Conclusion

The CELA team has made progress on a novel approach to spacecraft attitude control in the form of a magnetically levitated reaction sphere. We have developed a number of prototypes that test elements of the final design, and we are looking forward to future project phases leading to progressively more sophisticated devices. These prototypes include correlated electromagnetic circuit boards, hemispherical motors, spherical levitation test articles, LabVIEW and Arduino control software, MATLAB, Python, and COMSOL-based analysis, simulink control models, and 3D printing capabilities. We will continue to hone our management philosophy, build our team, and foster external collaborations. The project is multifaceted, and has been a learning process for each of us.

References

[1] Chakravorty, J., "Singularity avoidance in single gimbal CMG using the theory of potential functions," *Proceedings of the 10th World Congress on Intelligent Control and Automation*, 2012, pp. 1103–1108. https://doi.org/10.1109/WCICA.2012.6358045.

[2] Yoon, H., and Tsiotras, P., "Singularity Analysis and Avoidance of Variable-Speed Control Moment Gyros – Part I : No Power Constraint Case," 2004. https://doi.org/10.2514/6.2004-5207.

[3] Bialke, B., and Dorsey, G., "FUSE Reaction Wheel Torque Anomaly Resolution," *Advances in the Astronautical Sciences*, Vol. 107, 2001, pp. 441–458.

[4] Swann, M., "Diffusion of Magnetic Bearings," *Turbomachinery International Magazine*, 2009, pp. 30–32.

[5] Camacho, J. M., and Sosa, V., "Alternative method to calculate the magnetic field of permanent magnets with azimuthal symmetry," *Revista mexicana de física E*, Vol. 59, 2013, pp. 8–17.

[6] "NdFeB, Grade N52," https://www.kjmagnetics.com/proddetail.asp?prod=D44-N52, 2008. [Accessed: 2021-09-21].

[7] Rucker, C., "Integrating Rotations Using Nonunit Quaternions," *IEEE Robotics and Automation Letters*, Vol. 3, No. 4, 2018, pp. 2979–2986. https://doi.org/10.1109/LRA.2018.2849557.